

# 1 **Myocardial m<sup>6</sup>A regulators in postnatal development: effect of sex**

2 Dmytro Semenovych<sup>1,2</sup>, Daniel Benak<sup>1,2</sup>, Kristyna Holzerova<sup>1</sup>, Barbora Cerna<sup>2</sup>, Petr  
3 Telensky<sup>2,3</sup>, Tereza Vavrikova<sup>1,4</sup>, Frantisek Kolar<sup>1</sup>, Jan Neckar<sup>1</sup>, Marketa Hlavackova<sup>1,\*</sup>

4 <sup>1</sup>Laboratory of Developmental Cardiology, Institute of Physiology of the Czech Academy of  
5 Sciences, Prague, Czech Republic

6 <sup>2</sup>Department of Physiology, Faculty of Science, Charles University, Prague, Czech Republic

7 <sup>3</sup>International Clinical Research Center of St. Anne's University Hospital Brno, Dementia  
8 Research Group, Brno, Czech Republic

9 <sup>4</sup>Second Faculty of Medicine, Charles University, Prague, Czech Republic

10 \*Corresponding author: Marketa Hlavackova, Laboratory of Developmental Cardiology,  
11 Institute of Physiology of the Czech Academy of Sciences, Videnska 1083, 14220 Prague,  
12 Czech Republic. E-mail: [marketa.hlavackova@fgu.cas.cz](mailto:marketa.hlavackova@fgu.cas.cz)

## 13 **Summary**

14 N<sup>6</sup>-methyladenosine (m<sup>6</sup>A) is an abundant mRNA modification affecting mRNA stability and  
15 protein expression. It is a highly dynamic process, and its outcomes during postnatal heart  
16 development are poorly understood. Here we studied m<sup>6</sup>A machinery in the left ventricular  
17 (LV) myocardium of Fisher344 male and female rats (postnatal days one to ninety; P1-P90)  
18 using Western Blot. A downward pattern of target protein levels (demethylases FTO and  
19 ALKBH5, methyltransferase METTL3, reader YTHDF2) was revealed in male and female rat  
20 LVs during postnatal development. On P1, the FTO protein level was significantly higher in  
21 male LVs compared to females.

## 22 **Keywords**

23 Epitranscriptomics, N<sup>6</sup>-methyladenosine, Postnatal development, Heart

24 Epigenetic changes have significant importance during both heart development and the  
25 manifestation of heart diseases [1]. However, the role of epitranscriptomics, RNA epigenetics,  
26 has not yet been sufficiently explored in this area.

27 N<sup>6</sup>-methyladenosine (m<sup>6</sup>A) is the most prevalent internal chemical mark in mRNA. It is  
28 a dynamic and reversible modification that regulates RNA splicing, export from the nucleus,  
29 stability, and degradation [2]. The deposition of m<sup>6</sup>A methylation is mediated by proteins called  
30 “writers”. The most prominent one is methyltransferase-like 3 (METTL3), the catalytic subunit  
31 of a multicomponent methyltransferase complex [3]. In contrast, fat mass and obesity-  
32 associated protein (FTO) and alkB homolog 5 (ALKBH5) are “erasers” with the principal  
33 function of removing the m<sup>6</sup>A modification [4,5]. Besides m<sup>6</sup>A, FTO also demethylates m<sup>6</sup>Am,  
34 the main target of FTO in the cytosol, and N<sup>1</sup>-methyladenosine (m<sup>1</sup>A) in tRNA [6]. The  
35 biological functions of m<sup>6</sup>A are mediated by “readers” that bind to m<sup>6</sup>A-containing RNAs. YTH  
36 domain family 1-3 (YTHDF1-3) proteins are eminent m<sup>6</sup>A readers that all induce mRNA  
37 degradation [7]. The expression patterns of YTHDF paralogs differ across different cell types  
38 and tissues. Therefore, the dominant decay-inducing role is usually carried by the most  
39 abundant reader in particular cells. Importantly, YTHDF2 is often more highly expressed than  
40 YTHDF1 or YTHDF3 [7]. The m<sup>6</sup>A modification seems to have significant importance in the  
41 developing heart. Disruption in the proper functionality of m<sup>6</sup>A machinery proteins can lead to  
42 critical alterations in heart structure and function. For example, loss of enzymatic activity of  
43 FTO can lead to a ventricular septal defect, atrioventricular defect, and hypertrophic  
44 cardiomyopathy in humans [8]. Moreover, according to Su et al. [9], FTO levels drop in elderly  
45 murine hearts in response to acute myocardial ischemia/reperfusion injury, while those in young  
46 hearts are unaffected. The function of ALKBH5 is linked with an improvement in cardiac  
47 function and regeneration after myocardial infarction in juvenile and adult mice [10]. Recent  
48 reports also show progressive alterations in m<sup>6</sup>A levels during heart development [10-13].  
49 However, there is a lack of data regarding the detailed m<sup>6</sup>A machinery protein profiles in heart  
50 tissue during postnatal development and potential sex differences.

51 This pilot study aimed to investigate sex-specific changes in main m<sup>6</sup>A regulatory  
52 protein levels during postnatal development.

53 This study was conducted in accordance with the European Guidelines on Laboratory  
54 Animal Care. The use of animals was approved and supervised by the Animal Care and Use  
55 Committee of the Institute of Physiology of the Czech Academy of Sciences (No. 66/2021).

56 *Animals:* Fischer344 rats used for the experiments were bred and kept in the Faculty of  
57 Science of Charles University and sacrificed on postnatal days (P) 1, 4, 7, 10, 12, 14, 18, 21,  
58 25, 28, and 90 with n = 4-12 in each group (Table 1). The higher number of individual samples

59 in the early postnatal period was used because of their limited size. Rats were housed on a 12 h  
60 light/dark regime and were given unrestricted access to food and tap water.

61 *Tissue processing:* Hearts were dissected into the right ventricle (RV) and LV with septum and  
62 frozen in liquid nitrogen. Due to the limited size of the early postnatal LVs, all samples were  
63 grouped considering their age and sex and homogenized in eight volumes of ice-cold  
64 homogenization buffer (12.5 mM Tris, 2.5 mM EGTA, 250 mM sucrose, 6 mM  
65  $\beta$ -mercaptoethanol, pH 7.4) with the addition of the protease and phosphatase inhibitor cocktail  
66 (Roche Diagnostics, Switzerland) as described previously [14]. The protein concentration  
67 (Table 1) was measured using the Bradford assay (Bio-Rad, USA). Protein concentration was  
68 significantly lower at P1 compared to other days in both sexes. In males, the protein  
69 concentration increased gradually from P1 to P7, while in females there was a dramatic change  
70 between P1 and P4. The differences in protein concentration indicate significant changes in the  
71 ratio of dry mass to water in heart tissue in the early postnatal period. Our observation is in  
72 agreement with the already reported rapid postnatal decline in water content in heart tissue [15].

73 *Immunoblotting:* Proteins were separated by SDS-PAGE electrophoresis (10% gels) and  
74 transferred to polyvinylidene fluoride (PVDF) membranes (BioRad, USA; 1620177). The  
75 membranes were blocked using 5% dry low-fat milk in Tris-buffered saline with Tween 20  
76 (TBST) for 1 h at room temperature and incubated overnight at 4 °C with primary antibodies  
77 against: FTO [5-2H10] (Abcam, UK; ab92821, 1:1000), ALKBH5 [EPR18958] (Abcam, UK;  
78 ab195377, 1:1500), METTL3 [EPR18810] (Abcam, UK; ab195352, 1:1000), YTHDF2  
79 (Invitrogen, USA; PA5-70853, 1:1000). The membranes were subsequently incubated for 1 h  
80 at room temperature with secondary anti-rabbit (Bio-Rad, USA; 170-6515, 1:10000) or anti-  
81 mouse (Invitrogen, USA; 31432, 1:10000) antibodies. The chemiluminescence was measured  
82 by ChemiDoc™ System (Bio-Rad, USA). Ponceau S staining (Sigma-Aldrich, USA; P7170)  
83 was used as a loading control. It was shown as an effective way of normalization of samples of  
84 different developmental phases [16]. Both male and female protein levels were expressed as  
85 fold change over the corresponding P90 male signal (equal to 1). Female protein levels were  
86 recalculated to relevant P90 male signals to enable the quantification of sex-dependent  
87 differences.

88 *Statistics:* All statistical analyses were performed using GraphPad Prism 8 (GraphPad  
89 Software, Inc.). One-way ANOVA with Tukey's multiple comparisons test was used for the  
90 assessment of the statistical significance within sex. Two-way ANOVA with Tukey's multiple

91 comparisons test was used for the assessment of the statistical significance of sex differences.  
92 The data were obtained from at least three experiments and are displayed as means  $\pm$  standard  
93 deviation (SD). Results were recognized as statistically significant when  $P < 0.05$  (\* $P < 0.05$ ,  
94 \*\* $P < 0.01$ , \*\*\* $P < 0.001$ , \*\*\*\* $P < 0.0001$ ).

95 *Protein level profiles of m<sup>6</sup>A machinery during postnatal development in male and*  
96 *female hearts:* To investigate protein levels during postnatal development, we performed a  
97 western blot of LV tissue lysates collected from rats on postnatal days 1, 4, 7, 10, 12, 14, 18,  
98 21, 25, 28, and 90. We examined the erasers (FTO, ALKBH5), writer (METTL3), and reader  
99 (YTHDF2) proteins of m<sup>6</sup>A modification. YTHDF2 was chosen because of its highest  
100 expression among the paralogs in male LV (with the lowest Cq value indicating the highest  
101 gene abundance of *Ythdf2* ( $25.20 \pm 0.47$ ) compared to *Ythdf1* ( $25.91 \pm 0.25$ ) and *Ythdf3* ( $25.59$   
102  $\pm 0.64$ )). Firstly, we revealed that the abundance profile of all target proteins had a decreasing  
103 pattern during postnatal development (P1-P90) (Fig. 1). ALKBH5 and YTHDF2 declined  
104 dramatically between P1-P4 with further indistinct changes in protein levels. FTO and  
105 METTL3 protein expression dropped gradually throughout the investigated period. Concerning  
106 sex-related differences, it was found that the FTO level is significantly higher (by  $40.6 \pm 21.4\%$ )  
107 at P1 in males compared to females.

108 Our present study provides insights into the dynamics of m<sup>6</sup>A eraser, writer, and reader  
109 protein levels through postnatal development from P1 to P90 in rat left ventricles of both sexes.  
110 We showed that all proteins revealed a downward expression pattern with either a dramatic  
111 drop during the first critical period from P1 to P4 (ALKBH5 and YTHDF2) or a gradual decline  
112 till adulthood (FTO, METTL3). The decreasing patterns of METTL3 and ALKBH5 levels  
113 correspond to previously published reports [10,12]. Han et al. [10] utilized a mouse model and  
114 analyzed hearts at P1, P7, and P10. They showed the downregulation of protein and gene levels  
115 of ALKBH5 throughout this early developmental period. Also, Yang et al. [12] found a higher  
116 protein expression of ALKBH5 and METTL3 at P0 than at P7 in the rat heart, while the FTO  
117 level remained unchanged. In contrast, Yang et al. [13] found that the METTL3 level in mouse  
118 hearts is higher at P7 and P28 compared to P1. FTO protein level revealed a similar decreasing  
119 pattern as was observed in our study, its level at P1 was higher than at P7 and P28 [13]. Utilizing  
120 the porcine model, Ferenc et al. [17] showed differences in FTO expression between neonatal  
121 samples and adult ones in other tissues: skeletal muscle along with the thyroid gland and  
122 adipose tissue displayed the higher FTO signal in the neonatal period.

123 Interestingly, we observed that the FTO protein level in males is higher than in females  
124 at P1. The sex-dependent differences provoked by *Fto* level disruption were found in several  
125 reports. For example, sex-specific changes in body weight were observed upon overexpression  
126 of *Fto* in mice, with females showing a slightly higher weight gain than males [18]. At the time  
127 of weaning, both male and female *Fto* knockout mice were about 65% the weight of wild-type  
128 and heterozygous littermates. Nevertheless, *Fto* knockout male mice displayed persistent  
129 weight loss throughout their life, while female *Fto* knockout tended to make up the weight  
130 deficit by adulthood [19]. It may suggest a more significant role of FTO during the embryonic  
131 and early neonatal period in males that is in line with our data, where at P1 FTO level was  
132 higher in male samples than in female ones.

133 In conclusion, this study thoroughly assessed the protein levels of m<sup>6</sup>A machinery in rat  
134 LVs of both sexes during postnatal development. A downward pattern of all target protein levels  
135 was revealed in both sexes. Moreover, the FTO protein level was significantly higher in males  
136 compared to females on P1.

137

## 138 **Conflict of interest**

139 There is no conflict of interest.

## 140 **Funding**

141 The study was supported by the Charles University Grant Agency (grant number 1076119) and  
142 the Czech Science Foundation (grant number 19-04790Y).

## 143 **References**

- 144 1. Jarrell DK, Lennon ML, Jacot JG. Epigenetics and Mechanobiology in Heart Development and  
145 Congenital Heart Disease. *Diseases*. 2019;7(3)
- 146 2. Peer E, Rechavi G, Dominissini D. Epitranscriptomics: regulation of mRNA metabolism through  
147 modifications. *Curr Opin Chem Biol*. 2017;41:93-98.
- 148 3. Liu J, Yue Y, Han D, Wang X, Fu Y, Zhang L, Jia G, Yu M, Lu Z, Deng X, Dai Q, Chen W, He C. A METTL3-  
149 METTL14 complex mediates mammalian nuclear RNA N6-adenosine methylation. *Nat Chem Biol*.  
150 2014;10(2):93-95.
- 151 4. Jia G, Fu Y, Zhao X, Dai Q, Zheng G, Yang Y, Yi C, Lindahl T, Pan T, Yang YG, He C. N6-methyladenosine  
152 in nuclear RNA is a major substrate of the obesity-associated FTO. *Nat Chem Biol*. 2011;7(12):885-887.
- 153 5. Zheng G, Dahl JA, Niu Y, Fedorcsak P, Huang CM, Li CJ, Vågbø CB, Shi Y, Wang WL, Song SH, Lu Z,  
154 Bosmans RP, Dai Q, Hao YJ, Yang X, Zhao WM, Tong WM, Wang XJ, Bogdan F, Furu K, Fu Y, Jia G, Zhao  
155 X, Liu J, Krokan HE, Klungland A, Yang YG, He C. ALKBH5 is a mammalian RNA demethylase that impacts  
156 RNA metabolism and mouse fertility. *Mol Cell*. 2013;49(1):18-29.

- 157 6. Wei J, Liu F, Lu Z, Fei Q, Ai Y, He PC, Shi H, Cui X, Su R, Klungland A, Jia G, Chen J, He C. Differential  
158 m(6)A, m(6)A(m), and m(1)A Demethylation Mediated by FTO in the Cell Nucleus and Cytoplasm. *Mol*  
159 *Cell*. 2018;71(6):973-985.
- 160 7. Lasman L, Krupalnik V, Viukov S, Mor N, Aguilera-Castrejon A, Schneir D, Bayerl J, Mizrahi O, Peles S,  
161 Tawil S, Sathe S, Nachshon A, Shani T, Zerbib M, Kilimnik I, Aigner S, Shankar A, Mueller JR, Schwartz S,  
162 Stern-Ginossar N, Yeo GW, Geula S, Novershtern N, Hanna JH. Context-dependent functional  
163 compensation between Ythdf m(6)A reader proteins. *Genes Dev*. 2020;34(19-20):1373-1391.
- 164 8. Boissel S, Reish O, Proulx K, Kawagoe-Takaki H, Sedgwick B, Yeo GS, Meyre D, Golzio C, Molinari F,  
165 Kadhom N, Etchevers HC, Saudek V, Farooqi IS, Froguel P, Lindahl T, O'Rahilly S, Munnich A, Colleaux  
166 L. Loss-of-function mutation in the dioxygenase-encoding FTO gene causes severe growth retardation  
167 and multiple malformations. *Am J Hum Genet*. 2009;85(1):106-111.
- 168 9. Su X, Shen Y, Jin Y, Kim IM, Weintraub NL, Tang Y. Aging-Associated Differences in Epitranscriptomic  
169 m6A Regulation in Response to Acute Cardiac Ischemia/Reperfusion Injury in Female Mice. *Front*  
170 *Pharmacol*. 2021;12:654316.
- 171 10. Han Z, Wang X, Xu Z, Cao Y, Gong R, Yu Y, Yu Y, Guo X, Liu S, Yu M, Ma W, Zhao Y, Xu J, Li X, Li S, Xu  
172 Y, Song R, Xu B, Yang F, Bamba D, Sukhareva N, Lei H, Gao M, Zhang W, Zagidullin N, Zhang Y, Yang B,  
173 Pan Z, Cai B. ALKBH5 regulates cardiomyocyte proliferation and heart regeneration by demethylating  
174 the mRNA of YTHDF1. *Theranostics*. 2021;11(6):3000-3016.
- 175 11. Gong R, Wang X, Li H, Liu S, Jiang Z, Zhao Y, Yu Y, Han Z, Yu Y, Dong C, Li S, Xu B, Zhang W, Wang N,  
176 Li X, Gao X, Yang F, Bamba D, Ma W, Liu Y, Cai B. Loss of m(6)A methyltransferase METTL3 promotes  
177 heart regeneration and repair after myocardial injury. *Pharmacol Res*. 2021;174:105845.
- 178 12. Yang C, Zhao K, Zhang J, Wu X, Sun W, Kong X, Shi J. Comprehensive Analysis of the Transcriptome-  
179 Wide m6A Methylome of Heart via MeRIP After Birth: Day 0 vs. Day 7. *Front Cardiovasc Med*.  
180 2021;8:633631.
- 181 13. Yang Y, Shen S, Cai Y, Zeng K, Liu K, Li S, Zeng L, Chen L, Tang J, Hu Z, Xia Z, Zhang L. Dynamic Patterns  
182 of N6-Methyladenosine Profiles of Messenger RNA Correlated with the Cardiomyocyte Regenerability  
183 during the Early Heart Development in Mice. *Oxid Med Cell Longev*. 2021;2021:5537804.
- 184 14. Holzerová K, Hlaváčková M, Žurmanová J, Borchert G, Neckář J, Kolář F, Novák F, Nováková O.  
185 Involvement of PKCepsilon in cardioprotection induced by adaptation to chronic continuous hypoxia.  
186 *Physiological research*. 2015;64(2):191-201.
- 187 15. Solomon S, Wise P, Ratner A. Postnatal Changes of Water and Electrolytes of Rat Tissues.  
188 1976;153(2):359-362.
- 189 16. Sander H, Wallace S, Plouse R, Tiwari S, Gomes AV. Ponceau S waste: Ponceau S staining for total  
190 protein normalization. *Anal Biochem*. 2019;575:44-53.
- 191 17. Ferenc K, Pilzys T, Garbicz D, Marcinkowski M, Skorobogatov O, Dylewska M, Gajewski Z, Grzesiuk  
192 E, Zabielski R. Intracellular and tissue specific expression of FTO protein in pig: changes with age, energy  
193 intake and metabolic status. *Sci Rep*. 2020;10(1):13029.
- 194 18. Church C, Moir L, McMurray F, Girard C, Banks GT, Teboul L, Wells S, Brüning JC, Nolan PM, Ashcroft  
195 FM, Cox RD. Overexpression of Fto leads to increased food intake and results in obesity. *Nat Genet*.  
196 2010;42(12):1086-1092.
- 197 19. Gao X, Shin YH, Li M, Wang F, Tong Q, Zhang P. The fat mass and obesity associated gene FTO  
198 functions in the brain to regulate postnatal growth in mice. *PLoS One*. 2010;5(11):e14005.

199  
200

201

202 **Table 1.** The number of animals in pooled samples and concentration of total protein in  
 203 samples of male and female rat hearts.

Samples	Number of animals	Concentration ( $\mu\text{g}/\mu\text{l}$ )	SD
Males			
<b>P1</b>	11	5.39	0.96
<b>P4</b>	10	8.35	1.46
<b>P7</b>	4	10.81	0.06
<b>P10</b>	4	10.09	0.40
<b>P12</b>	5	10.62	1.25
<b>P14</b>	4	10.58	1.76
<b>P18</b>	5	12.07	0.13
<b>P21</b>	5	11.27	0.30
<b>P25</b>	5	11.92	0.40
<b>P28</b>	5	11.78	0.86
<b>P90</b>	4	13.23	1.85
Females			
<b>P1</b>	9	6.43	0.87
<b>P4</b>	12	11.82	1.92
<b>P7</b>	6	11.54	2.52
<b>P10</b>	6	10.18	1.58
<b>P12</b>	4	10.75	0.60
<b>P14</b>	5	10.47	1.76
<b>P18</b>	5	10.82	1.87
<b>P21</b>	5	10.32	1.44
<b>P25</b>	5	11.73	2.15
<b>P28</b>	5	12.37	0.96
<b>P90</b>	5	11.86	1.44

204 P – postnatal day; SD – standard deviation

205

206

207

208

209

210

211

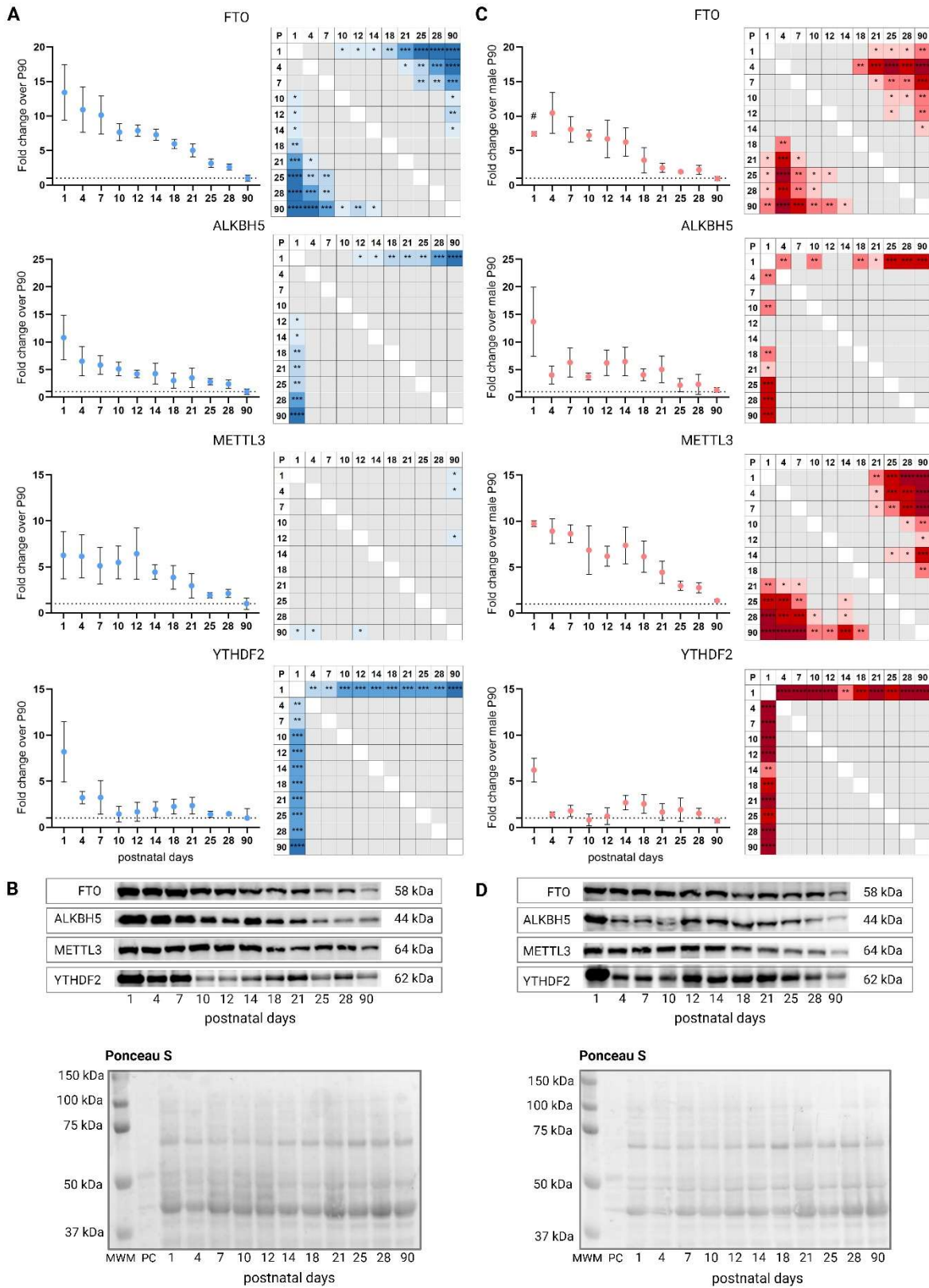
212

213

214 **Figure 1. The protein levels of the m<sup>6</sup>A regulators in male and female rat hearts.**  
215 A) Immunoblot analysis and multiple comparisons of the immunoblotting data of fat mass and  
216 obesity-associated protein (FTO), alkB homolog 5 (ALKBH5), methyltransferase-like 3  
217 (METTL3), and YTHDF2 (YTH domain family 2) in LV tissue homogenates from P1-P90  
218 male rats. B) Representative western blot membranes displaying FTO, ALKBH5, METTL3,  
219 and YTHDF2 protein levels in LV tissue homogenates from P1-P90 male rats and the  
220 representative total protein Ponceau S staining. C) Immunoblot analysis and multiple  
221 comparisons of the immunoblotting data of FTO, ALKBH5, METTL3 and YTHDF2 in LV  
222 tissue homogenates from P1-P90 female rats. D) Representative western blot membranes  
223 displaying FTO, ALKBH5, METTL3, and YTHDF2 protein levels in LV tissue homogenates  
224 from P1-P90 female rats and the representative total protein Ponceau S staining. Homogenates  
225 were pooled with n = 4-12 in each group (details in Table 1). All the protein expression levels  
226 were normalized to Ponceau S staining. Both male and female protein levels were expressed as  
227 fold change over the corresponding P90 male signal (equal to 1). Experiments were performed  
228 independently three times. Protein loading was 15 µg. \*P < 0.05, \*\*P < 0.01, \*\*\*P < 0.001,  
229 \*\*\*\*P < 0.0001 (One-way ANOVA; Tukey's multiple comparisons test). #P < 0.01 compared  
230 to corresponding P1 males (Two-way ANOVA with Tukey's multiple comparisons test).  
231 MWM – molecular weight marker, P – postnatal day, PC – positive control (rat brain).

232





233

234

**Fig. 1**